Sensors and Materials, Vol. 29, No. 9 (2017) 1259–1268
MYU Tokyo

S & M 1419

Optimization of Hydrogen Sensing Performance of Pt/WO_3 Gasochromic Film Fabricated by Sol–Gel Method

Hajime Takahashi, Shinji Okazaki,* Yoshiaki Nishijima, and Taro Arakawa

Faculty of Engineering, Yokohama National University,
79-5 Tokiwadai, Hodogaya-ku, Yokohama, Kanagawa 240-8501, Japan

(Received February 28, 2017; accepted May 9, 2017)

Keywords: hydrogen gas sensor, platinum-supported tungsten trioxide, gasochromism, optical transmittance change

The sensing performance of a sol–gel-derived Pt/WO_3 film used in an optical hydrogen gas sensor was evaluated and optimized. The Pt/WO_3 film was deposited on a quartz glass substrate by the sol–gel method based on the acidification of Na_2WO_3 aqueous solutions. Optical transmittance changes of the films as a result of exposure to hydrogen-containing gas were measured in the near-infrared region. The sensor performance was severely affected by fabrication parameters such as annealing conditions, precursor concentration, and catalyst loading. In the case of annealing at 500 °C, high sensitivity and fast response were obtained. An annealing time of at least 0.5 h was required to attain stable performance, and long annealing times had no effect on the sensitivity. However, the sensor performance and transparency of the film became poorer in the case of a ratio of over 0.4. The atomic ratio of Pt to W showed a considerable effect on the sensing characteristics. Both the sensitivity and response kinetics were promoted with increasing Pt loading. When the ratio was about 0.35, maximum sensitivity was observed. The concentration of the Na_2WO_4 solution used in the sol–gel process was also an important parameter. The sensitivity increased with increasing concentration since the thickness of the sensing film increased. The dependence of response speed on concentration was larger than that of recovery speed. When the film was exposed to H_2/N_2 gas, good response was observed; the hydrogen detection limit was about 0.001 vol% and minimal influence of water vapor was noted. The sensing performance, however, became poorer because oxygen inhibited the reaction when the film was exposed to hydrogen-containing air.

1. Introduction

As a countermeasure against global warming, a clean energy system using hydrogen has been attracting much attention. In a renewable energy system, hydrogen is produced from water by electrolysis which utilizes electricity generated by solar, wind, hydraulic, or geothermal power. However, areas where such natural resources are abundant are dispersed around the globe. To realize this energy system, technologies for safely transporting and storing a vast amount of hydrogen as the energy carrier are indispensable.

Hydrogen has a large diffusion coefficient because of its small molecular size, meaning that hydrogen gas easily leaks from storage containers and pipelines. Hydrogen gas also has highly

*Corresponding author: e-mail: okazaki-shinji-yp@ynu.ac.jp
http://dx.doi.org/10.18494/SAM.2017.1585

ISSN 0914-4935

explosive characteristics. In addition, it ignites with a very small input of energy in the hydrogen concentration above its lower explosion limit and the burning velocity is very high.[1,2] Therefore, the continuous, sensitive, and reliable monitoring of hydrogen leakage at storage or usage sites is required for reducing the risk of explosion. For example, a hydrogen sensor available in Europe gives a fast and reliable indication of danger at values of 20% of the lower explosion limit (0.8 vol%) and a final alarm at values of 40% (1.6 vol%).[3]

Thus, so far, various hydrogen gas sensors such as a thermochemical type,[4] a semiconductor type,[5] and others have been proposed and used. Among them, optical methods such as fiber-optic gas sensors have the advantages of being explosion-proof and immune to electromagnetic noise.[6]

Most optical sensors are based on changes in the optical properties of chemochromic materials such as palladium,[7] metal oxides,[8,9] metal hydrides,[10] and magnesium-containing alloys.[11] The coloration and bleaching of films upon exposure to a certain gas is defined as gasochromism, which recently have generated considerable attention for applications to smart windows[12] and gas sensors.[9] Tungsten trioxide using palladium or platinum as the catalyst for the dissociation of the hydrogen molecule is a typical candidate for a gasochromic material.[13] These films are nearly transparent in air atmosphere. They change to a dark blue color with exposure to hydrogen gas.[13] At room temperature, the gasochromic color reaction of a Pd- or Pt-loaded WO_3 film readily proceeds when the film is exposed to hydrogen gas.[12] The authors have been developing a hydrogen sensor device based on the sol–gel-derived platinum-supported tungsten trioxide (Pt/WO_3) thin film and have demonstrated its performance as a sensor.[9]

Many researchers reported that the gasochromic performance of WO_3 is severely influenced by fabrication parameters such as annealing conditions, catalyst loading, and others.[14–17] To achieve low-cost and high-performance sensors, further improvements and optimization of sensing film are needed. In this study, the dependence of the sensing characteristics of sol–gel-derived Pt/WO_3 film on the film-forming conditions was intensively evaluated. In addition, sensing performance in response to various conditions involving hydrogen gas was assessed.

2. Sensing Principle

The principle of the gasochromic reaction is described in the following equations.[18]

$$(x/2)H_2 \rightarrow xH_{ad} \rightarrow xH^+ + xe^- \quad (1)$$

$$WO_3 + xH^+ + xe^- \rightarrow H_xWO_3 \quad (2)$$

The color of the film is grayish and it is semitransparent in air. In the presence of hydrogen gas, hydrogen molecules dissociate on the Pt catalysts into hydrogen atoms (H_{ad}). Hydrogen ions and free electrons are formed through a spillover process. They react with tungsten trioxide to form a dark blue tungsten bronze in the color reaction. Therefore, the optical power transmitted through the film attenuates in a hydrogen-containing atmosphere.

In an oxidizing atmosphere, the regeneration of WO_3 results in bleaching [Eqs. (3) and (4)].[18]

$$(x/4)O_2 \rightarrow (x/2)O \quad (3)$$

$$H_xWO_3 + (x/2)O \rightarrow WO_3 + (x/2)H_2O \quad (4)$$

3. Sensor Fabrication and Experimental Setup

The experimental procedures for the sol–gel method to prepare sensing films are as follows. First, the sodium tungstate aqueous solution was passed through a cation exchange resin in hydrogen form. The resultant colloidal tungstic acid solution was mixed with a hexachloroplatinic acid solution and an ethanol/water solution. The amount of hexachloroplatinic acid solution used is related to the Pt/W ratio. The solution was then spin-coated (500 rpm, 5 min) on the substrate. The coating was dried at room temperature and annealed in air under different experimental conditions. X-ray diffraction (XRD) was used to investigate the crystal structure of the sensing films.

Figure 1 shows the experimental setup for evaluating the gasochromic behavior of Pt/WO_3 thin films. The test sample was placed in an airtight gas chamber with collimator lenses for transmittance measurements. These lenses were connected to a near-infrared laser-diode light source (1.3 μm, Anritsu Co., MG9001A) and an optical power meter through a transmission multimode optical fiber cable. The near-infrared light sources are widely utilized in fiber optics telecommunication systems. Therefore, the evaluation of sensing characteristics of the Pt/WO_3 film at this wavelength is important for assessing its applicability to advanced fiber-optic gas sensor devices. H_2/N_2 or H_2/air dry gas was used for hydrogen detection, and dry air was passed through for the recovery process. All experiments were conducted at room temperature.

Figure 2 shows a typical gasochromic response to hydrogen gas. The ordinate in the figure represents normalized optical power with respect to the steady-state transmitted power in air. The transmittance of the sample was high since the Pt/WO_3 film was semitransparent in air. When the film was exposed to hydrogen gas, the transmitted power sharply decreased and reached steady state. The coloration resulted from the high optical absorption coefficient of tungsten bronze formed by hydrogen reduction. In this study, the response width is defined as sensitivity. When the hydrogen-containing atmosphere was replaced with dry air, the recovery reaction proceeded. However, the recovery speed was slower than the response. To analyze this response kinetic, we also defined initial response and recovery rate as the slopes of the normalized response curves.

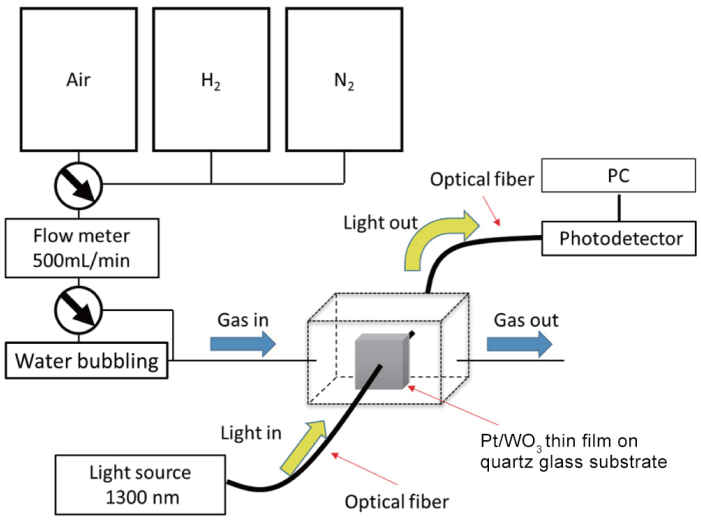

Fig. 1. (Color online) Experimental setup to measure change in transmittance caused by the gasochromic reaction.

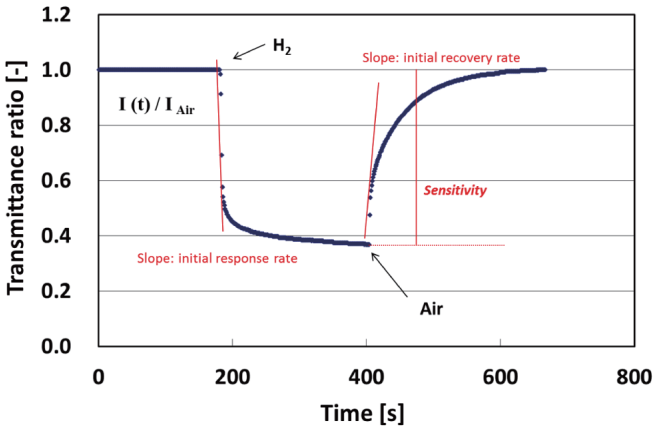

Fig. 2. (Color online) Typical gasochromic response to hydrogen gas.

4. Results and Discussion

4.1 Pt/W ratio

Figure 3 shows the effect of the Pt/W ratio on sensing performance. A strong dependence of the response curve on Pt/W ratio was observed. The sensitivity was enhanced by large Pt loadings and saturated in the high loading range. The response and recovery speed start to decrease with increasing Pt loading in the range exceeding this optimal ratio. It would result from the decrease in the effective reaction surface area with the progress of the aggregation of Pt catalyst particles in the dry annealing process. At high loading values above 0.4, the optical quality of the film deteriorated.

4.2 Precursor concentration

Figure 4 shows the effect of precursor concentration on sensing performance. A strong dependence of the response curve on precursor concentration was observed. Not only the sensitivity but also the reaction rate gradually increased with increasing concentration. It is suggested that the film is porous and this enhancement results from increasing film thickness. Generally, it is considered that the film thickness increases with increasing viscosity of the precursor solutions.[19] If the viscosity is positively correlated with the precursor concentration, the film thickness would increase with increasing concentration. It would result in an enhancement of the sensitivity and a reduction in the response speed since it takes much time to diffuse hydrogen gas into the inner region of the film. However, the response speed rather enhanced as shown in Fig. 4(b). Therefore, the film would have sufficient porosity to enable hydrogen gas molecules to easily pass through the film although such morphologies could not be observed from SEM images. This concentration dependence suggests that the sensor performances could be improved by increasing the precursor concentration. Owing to the large solubility of sodium tungstate (approximately 1.3 mol/L), further improvement would be possible in principle up to this limit value.

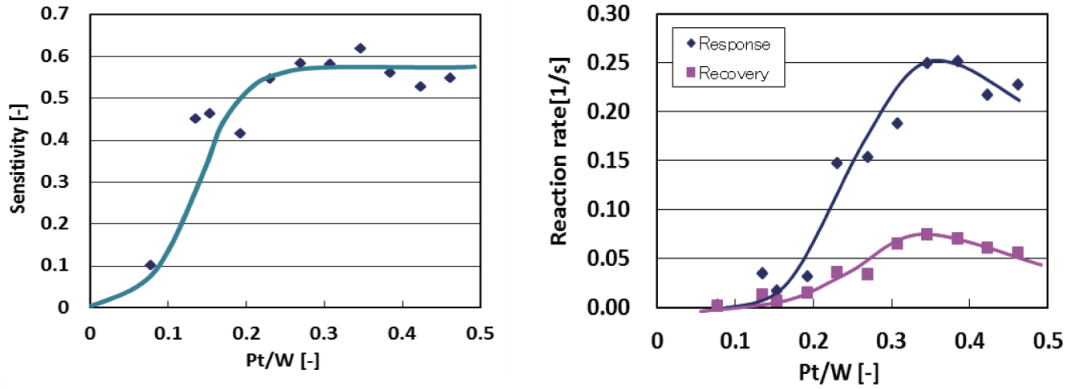

(a) (b)

Fig. 3 (Color online) Dependence of sensing parameters on Pt/W ratio. (a) Sensitivity and (b) reaction rate.

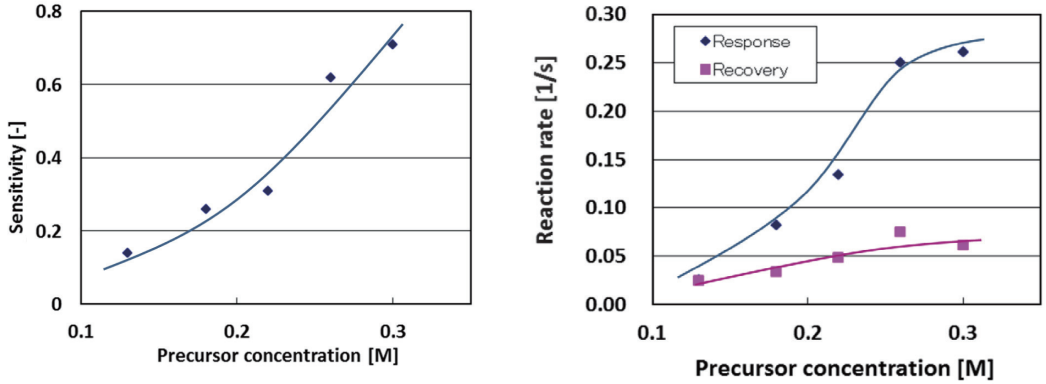

(a) (b)

Fig. 4. (Color online) Dependence of sensing parameters on precursor concentration. (a) Sensitivity and (b) Reaction rate.

4.3 Annealing temperature

Figure 5 shows the effect of annealing temperature on sensing performance. The effect of annealing temperature is somewhat complicated. For example, although the maximum value of sensitivity was obtained at 550 °C, the response kinetics at that temperature are relatively poor. Considering the trade-off, an annealing temperature ranging from 450 to 525 °C would be suitable for a sensor. The annealing temperature would affect both the crystal structure and morphology of the film. However, considerable changes in the morphology could not be detected in this experiment. Therefore, we mainly focused on the microscopic structural properties including WO_3 crystal growth and Pt segregation. To study these responses in more detail, XRD analysis was used to investigate the crystalline structure of the film. Figure 6 shows XRD patterns at different annealing temperatures. In the low-annealing-temperature region, sensitivity and reaction rate sharply increased. This suggests that many metallic platinum particles, which have a high catalytic activity, would be produced by the thermal decomposition of platinic acid during

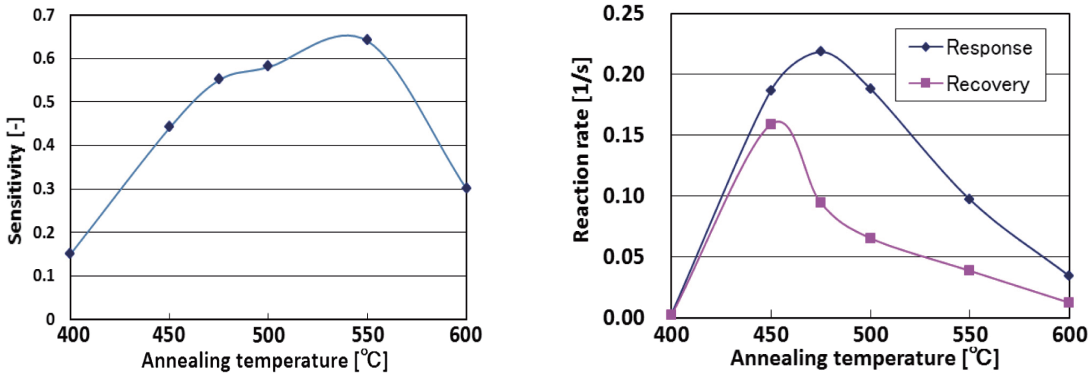

(a) (b)

Fig. 5. (Color online) Dependence of sensing parameters on annealing temperature. (a) Sensitivity and (b) reaction rate.

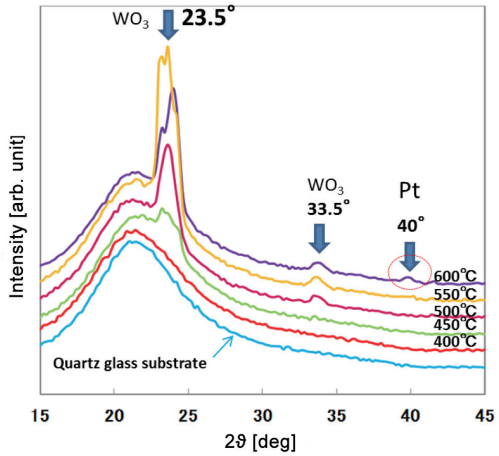

Fig. 6. (Color online) XRD patterns of Pt/WO_3 thin films at different annealing temperatures.

this annealing process. In the case of annealing at 400 °C, there was no peak. The other patterns show that crystalline WO_3 is formed when the annealing temperature is higher than 500 °C. We observed two main peaks. The lower-angle and strong peak around 23.5° seems to be composed of two or three distinct peaks. The intensities of these peaks increased as annealing temperatures were increased. In addition, a new small peak at 40° appeared in the XRD pattern at 600 °C. This peak must result from platinum. In addition, the agglomeration and the crystal growth of metallic platinum particles would also take place. This would inhibit the crystal growth of WO_3 as indicated by the decrease in the intensity of the peaks in the high-annealing-temperature region. The nanocrystalline WO_3 would be the dominant species under this optimal condition. Above this annealing temperature region, the crystallization of WO_3 readily proceeded, which led to an increase in coloration efficiency. On the other hand, a segregation of Pt simultaneously occurred and would result in a reduction of coloration rate.

4.4 Annealing time

Finally, the effect of annealing time on sensing performance was evaluated as shown in Fig. 7. At least 30 min of annealing was required to attain stable sensitivity, and longer annealing times had no effect on the sensitivity. In terms of response rate, annealing for 60 min was the best. The reproducibility of the sensor response could not be obtained in the case of an annealing time of less than 30 min. In the initial stage of annealing, not only crystal growth but also various physical and chemical phenomena occur. For example, the structural water preserved in the hydrate of WO_3 is discharged with the phase transition and the catalyst precursor decomposes to form platinum particles. In this case, the film would contain residual impurities such as water and chloride. It is indicated that these lead to the degradation of sensitivity and reaction rate due to catalyst poisoning.

In conclusion, optimum conditions for the preparation of Pt/WO_3 thin film were the following: Pt/W ratio, 0.35; precursor concentration, 0.3 M; annealing temperature, 500 °C; and annealing time, 60 min. Figure 8 shows the SEM image of the cross section of the film derived under these

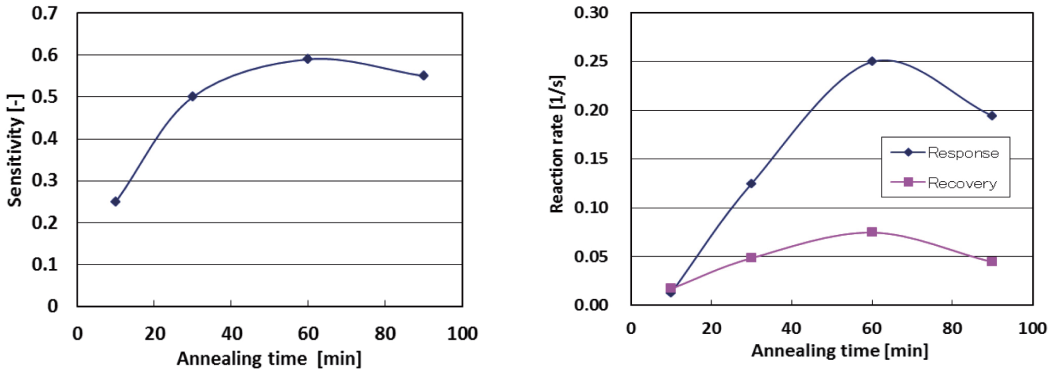

(a) (b)

Fig. 7. (Color online) Dependence of sensing parameters on annealing time. (a) Sensitivity and (b) reaction rate.

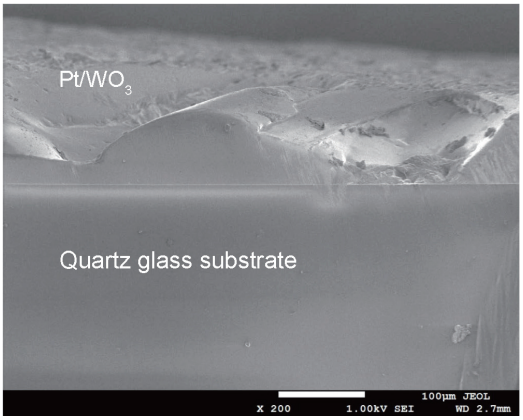

Fig. 8. SEM image of the cross section of Pt/WO_3 thin film derived within optimum conditions: Pt/W, 0.35; precursor concentration, 0.3 M; annealing temperature, 500 °C; and annealing time, 60 min.

conditions. Film thickness was 0.727 μm. The repeatability of the optical response of the film prepared under these conditions with 1% H_2/N_2 gas is shown in Fig. 9. This film also has good repeatability in response to a short period of measurement. Next, the detailed sensing performance of the thin film derived by this method was evaluated.

4.5 Sensing performance of the film under various conditions of hydrogen gas

Figure 10 shows sensing behavior for various concentrations of H_2/N_2 gas [Fig. 10(a)] and H_2/air [Fig. 10(b)]. According to Fig. 10, sensing performance depends on hydrogen concentration. In this study, the Pt/WO_3 thin film responded to 0.001% H_2/N_2 gas, while it responded to 0.1% H_2/air. That difference was caused by the presence of oxygen. When the film was exposed to H_2/air, both the color reaction [Eqs. (1) and (2)] and the bleaching reaction [Eqs. (3) and (4)] occurred simultaneously. Therefore, sensing performance was worse in H_2/air than in H_2/N_2 gas.

Then, the effect of water vapor on sensing performance was investigated. Humid hydrogen gas made by introducing water from a bubbler was introduced into the testing chamber, which was used to evaluate the sensing performance under wet conditions. Figure 11 shows the response to

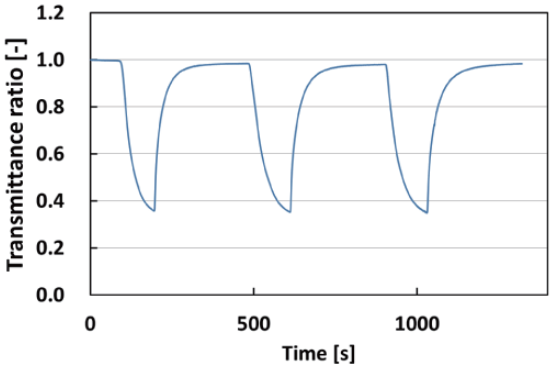

Fig. 9. (Color online) Repeatability of the optical response of Pt/WO_3 thin film derived within optimum conditions to 1% H_2/N_2 gas.

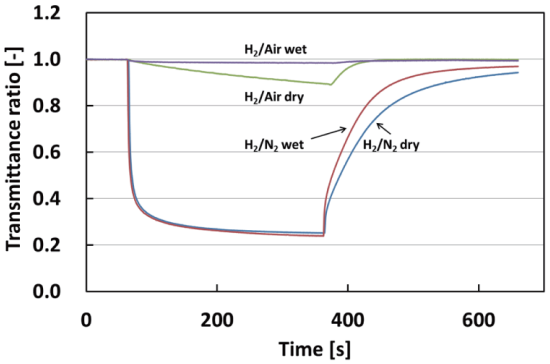

Fig. 11. (Color online) Response to 3% hydrogen gas under various conditions.

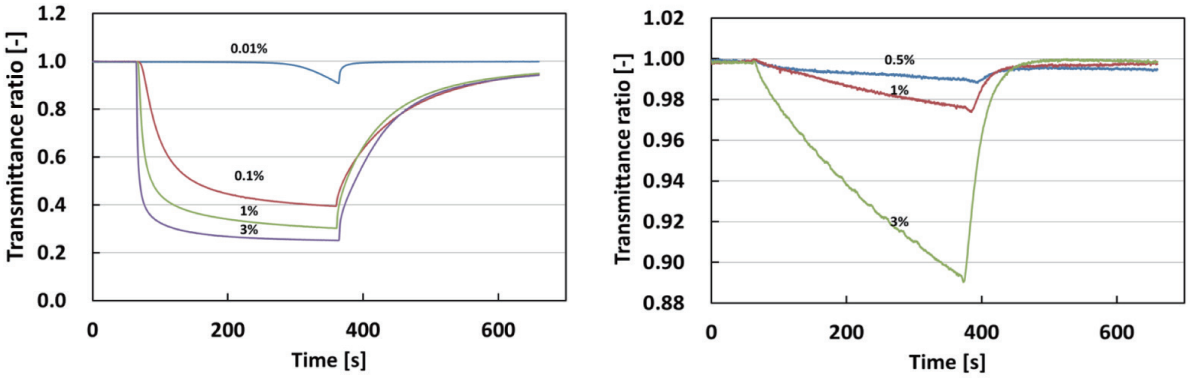

(a) (b)

Fig. 10. (Color online) Response of Pt/WO_3 thin film to various concentrations of hydrogen gas. (a) Response to H_2/N_2 gas and (b) response to H_2/air.

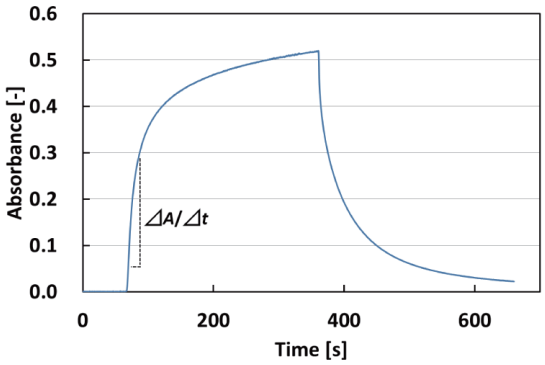

Fig. 12. (Color online) Absorbance change by introducing 1% H_2/N_2 gas.

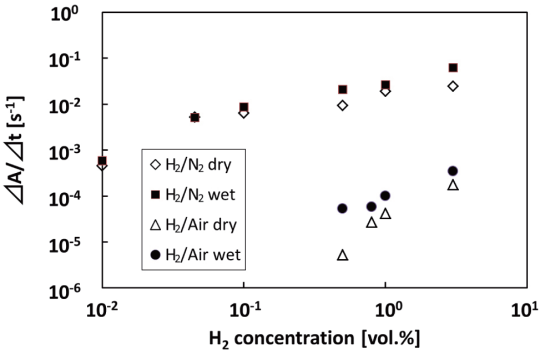

Fig. 13. Dependence of response rate on hydrogen concentration.

3% hydrogen gas under various conditions. The sensing performance to H_2/N_2 gas was slightly different between dry and wet conditions. On the other hand, recovery speed became faster. This means that moisture in hydrogen gas promotes bleaching [Eqs. (3) and (4)]. Therefore, sensing performance was worse in wet H_2/air than in dry H_2/air .

To evaluate the dependence of the response to hydrogen concentration quantitatively and to confirm the differences in the mechanism of response between several conditions, an analysis of response rates using the Beer–Lambert law [Eq. (5)] was carried out.

$$A = \log(I_{max}/I) = \varepsilon cL \tag{5}$$

(A: absorbance [-]; ε: absorption coefficient [L/(mol·cm)]; c: concentration of tungsten bronze [mol/L]; L: optical path length; I_{max}: transmitted light intensity at the baseline [-]; I: transmitted light intensity at the time [-])

The term I/I_{max} is normalized optical power. Absorbance was calculated as a result of taking the logarithm of the inverse value of the sensor output. By using Eq. (5), the response graph could be converted into absorbance–time graph (Fig. 12). Figure 13 shows the initial slope of the A–t curve ($\Delta A/\Delta t$) versus hydrogen concentration. The reaction order of the gasochromic reaction can be obtained from the slopes of the approximate straight lines in the plots in Fig. 13 because A is proportional to c if ε and L are constants in Eq. (5). Figure 13 confirms these facts. First, response rates depended on hydrogen concentration. Second, the response mechanism when the film was exposed to H_2/N_2 gas was different from that when H_2/air was introduced into the testing chamber; the reaction order of the response to H_2/N_2 gas was about 0.5 and that to H_2/air was about 1.0. Hydrogen sensors are used in the presence of oxygen, so response inhibition by oxygen is a serious problem that must be overcome.

5. Conclusions

The dependence of gasochromic characteristics on the parameters in the sol–gel method was intensively studied. The effects of parameters such as annealing conditions and catalyst loading in the fabrication process on sensor performance were evaluated. When the atomic ratio of Pt to W was about 0.35, maximum performance was obtained. The sensor performance and transparency

of the film deteriorated when the ratio was over 0.4. The sensitivity was enhanced when the precursor concentration was increased because the thickness of the sensing film increased. In the case of annealing at 500 °C, high sensitivity and fast response were obtained. At least 30 min of annealing time was required to attain stable performance, and long annealing times had no effect on sensitivity.

The sensing performance of films to various concentrations of hydrogen gas under dry/wet conditions was also studied. When the film was exposed to H_2/air, the sensing performance degraded compared with that when it was exposed to H_2/N_2 gas because oxygen in air caused a bleaching reaction in the response. Optical measurements in a wet atmosphere revealed that water vapor promoted the bleaching reaction. Response rates were analyzed to quantify the dependence of the optical response of the film on hydrogen concentration and to confirm the different mechanisms of gasochromic reaction in response to H_2/N_2 gas and H_2/air. More study is needed to remove the effect of the reverse reaction on sensing performance in the response process.

References

1 G. R. Astbury: Process Saf. Environ. Prot. **86** (2008) 397.
2 D. A. Crowl and Y. D. Jo: J. Loss Prev. Process Ind. **20** (2007) 158.
3 S. Linke, M. Dallmer, R. Werner, and W. Moritz: Int. J. Hydrogen Energy **37** (2012) 17523.
4 C. Han, D. Hong, S. Han, J. Gwak, and K. C. Singh: Sens. Actuators, B **125** (2007) 224.
5 T. Rashid, D. Phan, and G. Chung: Sens. Actuators, B **185** (2013) 777.
6 X. Zhou, Y. Dai, M. Zou, J. M. Karanja, and M. Yang: Sens. Actuators, B **236** (2016) 392.
7 R. Gupta, A. A. Sagade, and G. U. Kulkarni: Int. J. Hydrogen Energy **37** (2012) 9443.
8 A. Wisitsoorat, M. Z. Ahmad, M. H. Yaacob, M. Horpratum, D. Phakaratkul, T. Lomas, A. Tuantranont, and W. Wlodarski: Sens. Actuators, B **182** (2013) 795.
9 S. Okazaki, H. Nakagawa, S. Asakura, Y. Tomiuchi, N. Tsuji, H. Murayama, and M. Washiya: Sens. Actuators, B **93** (2003) 142.
10 M. M. H. Bhuiya, A. Kumar, and K. J. Kim: Int. J. Hydrogen Energy **40** (2015), 2231.
11 K. Yoshimura, S. Bao, N. Uchiyama, H. Matsumoto, T. Kanai, S. Nakabayashi, and H. Kanayama: Vacuum **83** (2008) 699.
12 W. Feng, L. Zou, G. Gao, G. Wu, J. Shen, and W. Li: Sol. Energy Mater. Sol. Cells **144** (2016) 316.
13 M. H. Yaacob, M. Z. Ahmad, A. Z. Sadek, J. Z. Ou, J. Campbell, K. Kalantar-zadeh, and W. Wlodarski: Sens. Actuators, B **177** (2013) 981.
14 J. Diaz-Reyes, R. J. Delgado-Macuil, V. Dorantes-Garcia, A. Perez-Benitez, J. A. Balderas-Lopez, and J. A. Ariza-Ortega: Mater. Sci. Eng., B **174** (2010) 182.
15 X. Sun, H. Cao, Z. Liu, and J. Li: Appl. Surf. Sci. **255** (2009) 8629.
16 J. Z. Ou, M. H. Yaacob, M. Breedon, H. D. Zheng, J. L. Campbell, K. Latham, J. du. Plessis, W. Wlodarski, and K. Kalantar-zadeh: Phys. Chem. Chem. Phys. **13** (2011) 7330.
17 C. C. Chan, W. C. Hsu, C. C. Chang, and C. S. Hsu: Sens. Actuators, B **145** (2010) 691.
18 T. Watanabe, S. Okazaki, H. Nakagawa, K. Murata, and K. Fukuda: Sens. Actuators, B **145** (2010) 781.
19 Y. Takahashi and Y. Matsuoka: J. Mater. Sci. **23** (1988) 2259.